Monolayer and Brewster Angle Microscopy Studies of Poly(methyl methacrylate)−Monopalmitin Mixed Systems at the Air−Water Interface

Mercedes Miñones Conde,[‡] J. M. Trillo,[†] Olga Conde,[†] and Jose Miñones, Jr.*

Department of Physical Chemistry, Faculty of Pharmacy, and Department of Optometry, School of Optics and Optometry, University of Santiago de Compostela, Campus Sur., 15706-Santiago de Compostela, Spain

Received: August 15, 2009; Revised Manuscript Received: December 2, 2009

Mixed monolayers of poly(methyl metacrylate) (PMMA) and monopalmitin (Mp) were used for the study of their interactions. A thorough analysis of surface pressure (π)−area (A) isotherms with the Langmuir monolayer technique, complemented with Brewster angle microscopy (BAM) images was performed. Mixed films show two phase transitions at a surface pressure of 14.5 mN/m and at 20−21 mN/m, respectively. Moreover, mixed monolayers show two well-defined collapses: one, corresponding to the lipid (at surface pressures of 50−51 mN/m) and the another one, ascribed to the PMMA, at surface pressure values of 57−58 mN/m. When the mean molecular areas of the mixed films ($A_{1,2}$) were plotted versus film composition (X_1 or X_2), positive deviations from the ideal behavior were observed at surface pressures below 15 mN/m, which were mainly attributed to a change in the conformation of the PMMA molecules at the surface. However, at higher surface pressures, the areas per monomer unit of the mixed monolayers obey the additivity rule, attributed to the fact that the film components form an immiscible system in these conditions.

1. Introduction

The studies between polymers and biocomponents in monolayers have awakened increasing interest in recent years due to their potential relevance to medical and pharmaceutical fields. So, with regard to regarding to medical applications, polymers such as PMMA (and other related compounds) are the main components of the contact lenses, whose use for the correction of ametropia problems (especially myopia) is increasing exponentially, estimating that about one hundred million people usually use this type of lens. Furthermore, this number is growing considerably, so it is expected that shortly this should exceed the number of conventional lenses (glasses) users.

On the other hand, it is well-known the resistance conferred by blood ocular barriers against the penetration of drugs across them,[1,2] so that very high drug doses are required to achieve adequate efficacy in the treatment of different eye diseases and injuries, often related to infections, allergic reactions, vascular alterations (glaucoma) and degenerative processes.[3,4] However, this requirement can lead to an increased probability of significant side effects, especially when patients are subjected to chronic treatments. Therefore, the pharmaceutical industry is very interested in the research of new ocular drug administration systems. In recent years, the idea of employing contact lenses as a drug reservoir[5] has awakened increasing interest, since the possibility of correcting a vision problem and simultaneously treat an ocular disease pharmacologically, is undoubtedly appealing.[6] Furthermore, the daily use of contact lenses involves a non-negligible risk, estimated in 25% of the cases, of causing erosions and infections in the eye that could be reduced by the use of medicated contact lenses.[7−9]

Many of these problems associated with the continuous use of contact lenses involves can be caused by the interactions occurring between the polymer constituting constituent of the contact lens and the components of the ocular tears. To our knowledge, no report on these molecular interactions has been carried out, and consequently, given their importance, we should study their existence, thereby using the Langmuir film balance technique. For this purpose, in this paper we begin to study the behavior of mixed monolayers that are made, on the one hand, of poly(methyl methacrylate) (PMMA) (the main component of the hard contact lenses and whose monomer is an essential constituent of the oxygen-permeable hydrophilic soft contact lenses, with high and low water content) and, on the other, of monopalmitin (a glyceride component of the tears), so that this monolayer is an in vitro model of the optical lens in contact with the eye. With this simple model, the analysis of surface−area pressure isotherms (π−A) obtained by compression of the mixed monolayers allows us to determine the behavior (interactions) of the mixed system.

2. Experimental Section

Syndiotactic PMMAs of molecular weights M_w = 15 000 and 120 000 g/mol were purchased from Aldrich (purity 95%) and used without further purification. Monopalmitin was supplied by Sigma (purity 99%). The storage of these materials was made according to the supplier information. Spreading solutions were prepared by weighing a proper amount (typically 2−3 mg) of the investigated compound on the analytical balance (accurate to 0.1 mg) and dissolving each compound in chloroform. Mixed solutions were prepared from the respective stock solutions of both compounds. The number of molecules spread on water subphase was 8.5×10^{16}.

Ultrapure water used as a subphase was obtained from a Milli-Ro, Milli-Q reverse osmosis system (Millipore Corp.), with a resistivity of 18.2 MΩ cm. Surface pressure−area isotherms were recorded with a KSV (Finland) Langmuir trough (total area = 850 cm^2) placed on an isolated vibration-free table and enclosed in a glass chamber to avoid contaminants from the

* To whom correspondence should be addressed. Phone: +34 981 563100. Ext. 14917. Fax: +34 981 594912. E-mail: qf.minones@usc.es.
‡ Department of Optometry.
† Department of Physical Chemistry.

10.1021/jp907900g
Published on Web 02/02/2010

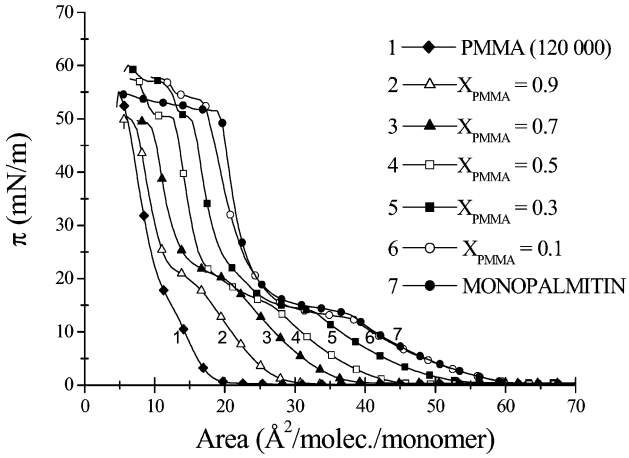

Figure 1. Surface pressure (π)−area (A) isotherms of PMMA (M_w = 120 000)−monopalmitin mixed monolayers spread on water (pH 6 at 30 °C).

air. Regulation of the trough temperature was controlled by circulating constant temperature water from a Haake thermostat through the tubes attached to the aluminum-based plate of the trough. The subphase temperature was measured by a thermocouple located just below the air/water interface. Two barriers confining the monolayer at the interface were driven symmetrically at a constant speed of 4.2 Å^2 molecules^{-1} min^{-1} during the film compression. This is the highest value for which isotherms have been found to be reproducible in preliminary experiments. Surface pressure was measured with an accuracy of ±0.1 mN/m using a Wilhelmy plate made from platinum foil as a pressure sensor. After spreading, monolayers were left for 10 min to ensure the solvent evaporation of the solvent.

To observe the morphological characteristics of the monolayer at the air−water interface by Brewster angle microscopy (BAM), a large trough constructed by Nima Technology Ltd., U.K. (model 601 BAM) was used. The trough has a working area of 70 cm × 7 cm, which is large enough to mount the BAM directly on it. BAM images and ellipsometric measurements were performed with BAM 2 Plus (NFT, Göttingen, Germany) equipped with a 30 mW laser emitting p-polarized light with a wavelength of 532 nm which was reflected off the air/water interface at approximately 53.1° (incident Brewster angle). Under such condition, the reflectivity of the beam was almost zero on the clean water surface. The reflected beam passes through a focal lens into an analyzer at a known angle of incident polarization, and finally to a CCD camera.

3. Results

3.1. Synd-PMMA (120 000)−Monopalmitin Mixed Monolayers. ***3.1.1. π−A Isotherms.*** At 30 °C, the π−A isotherm of *synd*-PMMA (M_w = 120 000) shows the existence of an inflection at a surface pressure about of approximately 17 mN/m (Figure 1, curve 1), similar to the one obtained by Hsu et al.[10] for the polymer with a molecular weight of 100 000 g/mol. In our view, this inflection or pseudoplateau corresponds to a LE−L′E phase transition of the monolayer from a *liquid-expanded* (LE) state to another one (L′E), which is slightly less compressible, as mentioned further below.

In the range between 60 and 70 Å^2/molecule, the monopalmitin monolayer (Figure 1, curve 7) exhibits a *gas−liquid expanded* phase transition (G−LE). For areas below 60 Å^2/molecule, the monolayer shows first a *liquid-expanded* (LE) state and then (at approximately 50 Å^2/molecule) a phase transition from the *liquid-expanded* state to the *liquid-condensed* one (LE−LC). This transition occurs at a surface pressure about of approximately 14.5 mN/m, and it takes a plateau-like shape in the corresponding π−A isotherm.

Isotherms of monopalmitin-rich mixtures (X_{PMMA} = 0.1 and 0.3) show the same plateau at surface pressures (14.5 mN/m), which hardly vary with the composition of the mixed film. In the isotherms of PMMA-rich mixtures (X_{PMMA} = 0.7 and 0.9) there is no such plateau, but the presence of another one is observed at surface pressures in the range 19−21 mN/m, a value slightly higher than in the π−A curve of pure PMMA.

The monolayer corresponding to the equimolar mixture shows an intermediate behavior in which the two above-mentioned plateaus coexist: the first at 14.5 mN/m and the other at 20 mN/m, that is, at the same surface pressures at which phase transitions of pure components occur.

At high surface pressures, the mixed monolayers exhibit two collapses: the first coinciding with the one of pure monopalmitin (at a surface pressure value around 50−51 mN/m) and the other coinciding with the one characteristic of the PMMA, at surface pressure values about of approximately 58 mN/m. These two collapses can be seen clearly in the curves corresponding to the monolayers of composition X_{PMMA} = 0.1−0.5. When the polymer content is higher than 0.5, only the monopalmitin collapse is observed. The one specific to the polymer cannot be observed, since the area where the increased pressure of the monolayer ("lift-off"area) can be detected is very small (below 40 Å^2/molecule). Consequently, in this situation, the mobile barrier compressing the film is very close to the place where the surface pressure-measuring plate is installed on the surface balance. As a result, it is impossible to compress the monolayer until reaching its second collapse, since before reaching it, the mobile barrier gets to reach the end of its pathway.

3.1.2. Compressional Modulus (C_s^{-1})−Surface Pressure (π) Plots. This type of representation enables us to check more precisely the surface state specific of monolayers and to see how it varies when changing the composition of the components in the mixture. The C_s^{-1}−π curve of pure monopalmitin shows a minimum value (M_1) at a surface pressure of 14.5 mN/m (Figure 2A), which verifies the existence of the pseudoplateau described in the π−A isotherm of this component (Figure 1, curve 7), attributed, as we have just mentioned, to the phase transition from a *liquid-expanded* to a *liquid-condensed* state. Once the minimum value of C_s^{-1} was exceeded, the compressional modulus increases as the monolayer is compressed to a maximum value of 191.4 mN/m, confirming the existence of a *liquid-condensed* state under these conditions.

C_s^{-1}−π curves of mixed monolayers with a higher monopalmitin content (X_{PMMA} = 0.1 and 0.3) also exhibit the existence of a significant minimum value (M_1) at surface pressures basically equal to those of the pure lipid (π_t = 14.5 mN/m), which do not vary significantly with the composition of the mixed film (Figure 2A). In addition to this minimum, the presence of another, M_2 (less pronounced), is observed at surface pressures about of approximately 19−21 mN/m, but without perceiving the existence of the corresponding plateau at these pressure values in the π−A isotherms. This demonstrates the importance of the compressional modulus plots, which allow the observation of monolayer phase transitions, which cannot be visualized in the corresponding compression isotherms.

C_s^{-1}−π curves of mixed monolayers with a higher PMMA content (X_{PMMA} = 0.7 and 0.9) (Figure 2C) exhibit only the second minimum (M_2) of the two described above, which

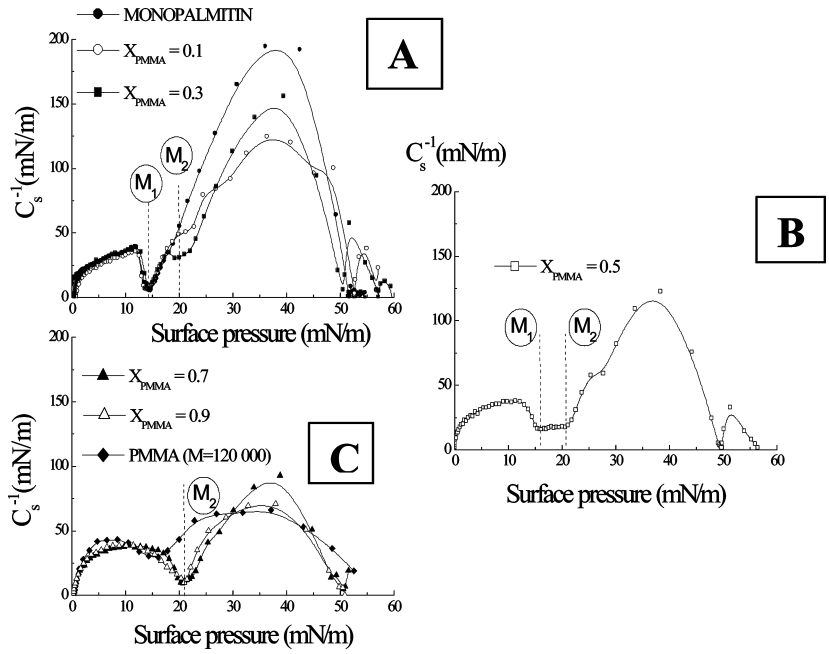

Figure 2. Compressional modulus (C_s^{-1})−surface pressure (π) plots for pure components and for mixed PMMA (M_w = 120 000)−monopalmitin monolayers spread on water at pH 6 and 20 °C. (A) Monopalmitin and mixtures of X_{PMMA} = 0.1 and 0.3 content. (B) Mixed monolayers of equimolar composition. (C) PMMA and mixed monolayers with high polymer content.

TABLE 1: Surface Pressure Values Corresponding to Different Phase Transitions of PMMA (M_w = 120 000)−Monopalmitin Mixed Monolayers Spread on Water at pH 6 and 30 °C

X_{PMMA}	first phase transition (mN/m)	second phase transition (mN/m)	first collapse (mN/m)	second collapse (mN/m)
0	14.5		51.5	
0.1	14.3	21.2	52.6	56.7
0.3	14.5	19.6	50.8	57.0
0.5	15.5	20.5	50.5	57.3
0.7		20.6	50.9	
0.9		20.9	50.8	
1		17.0		58.5

appears at surface pressure values between 20 and 21 mN/m, regardless of the mixture composition.

Finally, the film corresponding to X_{PMMA} = 0.5 shows the peculiar behavior described above: the $C_s^{-1}-\pi$ curve exhibits a region with minimal elasticity that extends along a range of surface pressures between 15 and 20.5 mN/m (Figure 2B).

At surface pressures lower than 20 mN/m all mixed monolayers are in an expanded state, with the compressional modulus below 50 mN/m. However, at higher surface pressures the monopalmitin-rich films are in a *liquid-condensed* state, with maximum values of the compressional modulus about of approximately 190 mN/m, whereas the PMMA-rich films have C_s^{-1} values below 100 mN/m, thus continuing to be in an expanded state.

The surface pressure values for the phase transitions of the pure films and the different mixtures, obtained from the $C_s^{-1}-\pi$ plots, are shown in Table 1.

3.1.3. Mean Molecular Area−Mole Fraction Plots. Figure 3 shows the plots of the mean molecular area of the mixed monolayers according to the PMMA mole fraction. The area values have been measured at different surface pressures: at π = 5and 10 mN/m, that is, below the first plateau of the $\pi-A$ curves, and at π = 25 and 30 mN/m, above the second phase transition.

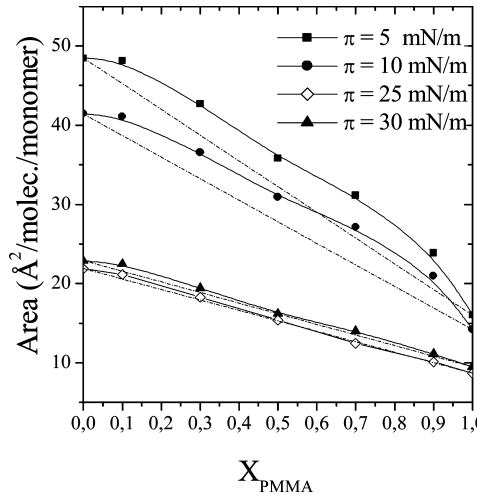

Figure 3. Mean molecular area vs mole fraction plots for PMMA (M_w = 120 000)−monopalmitin mixed monolayers at different surface pressures. Subphase: water, pH 6 at 30 °C. Dashed lines: ideal behavior. Solid lines: experimental results.

At surface pressures of 5 and 10 mN/m (when the mixed films exhibit an expanded state), positive deviations from the ideal behavior are observed. However, at higher surface pressure (π = 25 or 30 mN/m) the experimental results match up with the theoretical values calculated from the additivity rule: $A_m = X_{PMMA}A_{PMMA} + X_{MP}A_{MP}$. This behavior is typical for ideal mixed monolayers formed by miscible components or for systems of immiscible components at the air−water interface. In the first case, the collapse pressure of the mixed monolayers should vary with their composition, whereas in the second each component must collapse at its own surface pressure, regardless of the presence of the other. The results in Figure 1 show that the mixed monolayers undergo two collapses, which is also confirmed considering the results for the plot of the compressional modulus versus the composition of mixed systems (Figure

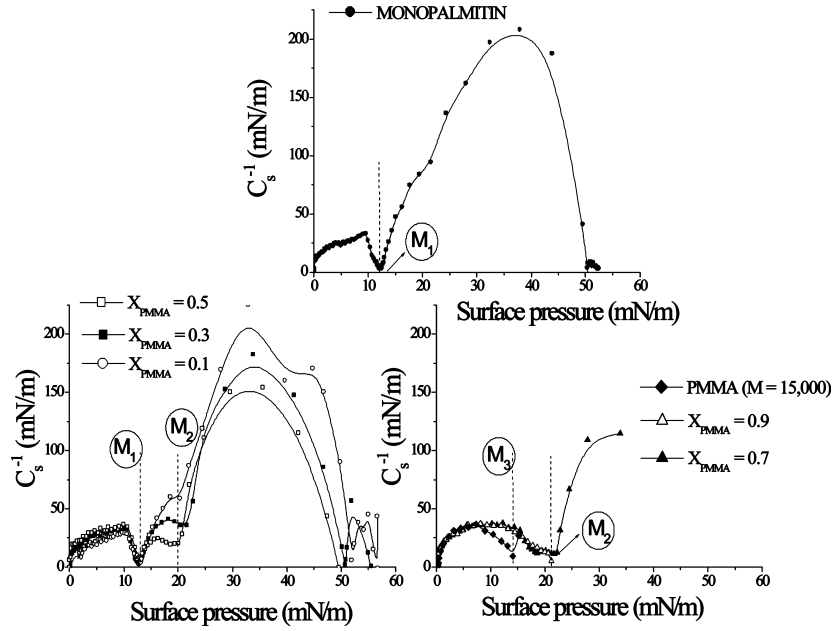

Figure 4. Compressional modulus (C_s^{-1})−surface pressure (π) plots for pure components and for mixed PMMA (M_w = 15 000)−monopalmitin monolayers spread on water, pH 6 and 30 °C.

2), where two minimal values, typical for high surface pressures, about 50 mN/m (collapse pressure of monopalmitin) and 58 mN/m (collapse pressure of PMMA) were observed. Consequently, we can consider that at high surface pressures, components are immiscible in the mixed monolayer, which leads to the linearity of the molecular areas.

3.2. Synd-PMMA (15 000)−Monopalmitin Mixed Monolayers. ***3.2.1. Compressional Modulus (C_s^{-})^1−Surface Pressure (π) Curves.*** A behavior similar to the one described above is observed when the mixed monolayers are made of *synd*-PMMA with a molecular weight of 15 000. In this case the study was conducted in a Nima balance where the BAM microscope was installed. For space reasons $\pi-A$ isotherms of these monolayers are not shown; we merely describe the $C_s^{-1}-\pi$ curves (Figure 4), where we can accurately observe the surface pressure values at which the phase transitions of the films occur. Two minimal values are clearly observed in the elasticity curves. The first one (M_1) is given only in mixtures where the PMMA proportion is $X_{PMMA} = 0.1-0.5$, where its surface pressure does not basically depend on the composition of the mixed monolayer. The second minimum (M_2) is observed for all monolayers, and the surface pressure at which it occurs (20−21 mN/m) does not depend on the mole fraction of the mixture. (M_3) is the minimum corresponding to pure the PMMA (15 000) monolayer.

The surface pressure values obtained for the two phase transitions (LE−LC of the lipid and LE−L′E of the polymer), as well as the collapse surface pressure values, are shown in Table 2.

3.2.2. Mean Molecular Area−Mole Fraction Plots. Figure 5 shows the plots of the mean molecular areas of the mixed monolayers versus the mole fraction of PMMA. The behavior of the M_w = 15 000 polymer is similar to that described for PMMA (M_w = 120 000): at surface pressures below the first phase transition of the mixed monolayers (π < 15 mN/m) there are positive deviations from the ideal behavior, although lower than for the PMMA (120 000)−Mp system. At surface pressures higher than that those corresponding to the second phase transition (π > 20 mN/m) the A_m-X_{PMMA} plots are linear.

3.2.3. Thickness−Time Plots and BAM Images. Figure 6 shows $d-t$ (thickness/time) plots of *synd*-PMMA (M_w = 15 000)

TABLE 2: Surface Pressure Values Corresponding to Different Phase Transitions of PMMA (M_w = 15 000)−Monopalmitin Mixed Monolayers Spread on Water at pH 6 and 30 °C

X_{PMMA}	first phase transition (mN/m)	second phase transition (mN/m)	first collapse (mN/m)	second collapse (mN/m)
0	12.5		50.8	
0.1	12.5	20.5	50.7	55.2
0.3	12.7	20.5	50.6	55.6
0.5	12.6	20.5	50.8	
0.7		21		
0.9		20.7		
1				

and monopalmitin mixtures of different compositions. The results for the mixture of X_{PMMA} = 0.9 were not included because with the number of molecules spread at the interface, the barrier that compresses the film reaches the end of its pathway before getting to the full range of the $\pi-A$ isotherm of this mixture.

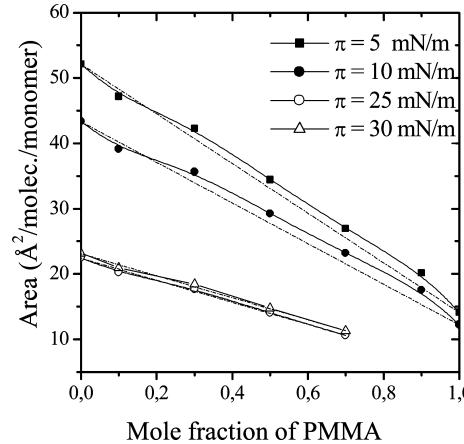

Figure 5. Mean molecular area vs mole fraction plots for PMMA (M_w = 15 000)−monopalmitin mixed monolayers at different surface pressures. Subphase: water, pH 6 at 30 °C. Dashed lines: ideal behavior. Solid lines: experimental results.

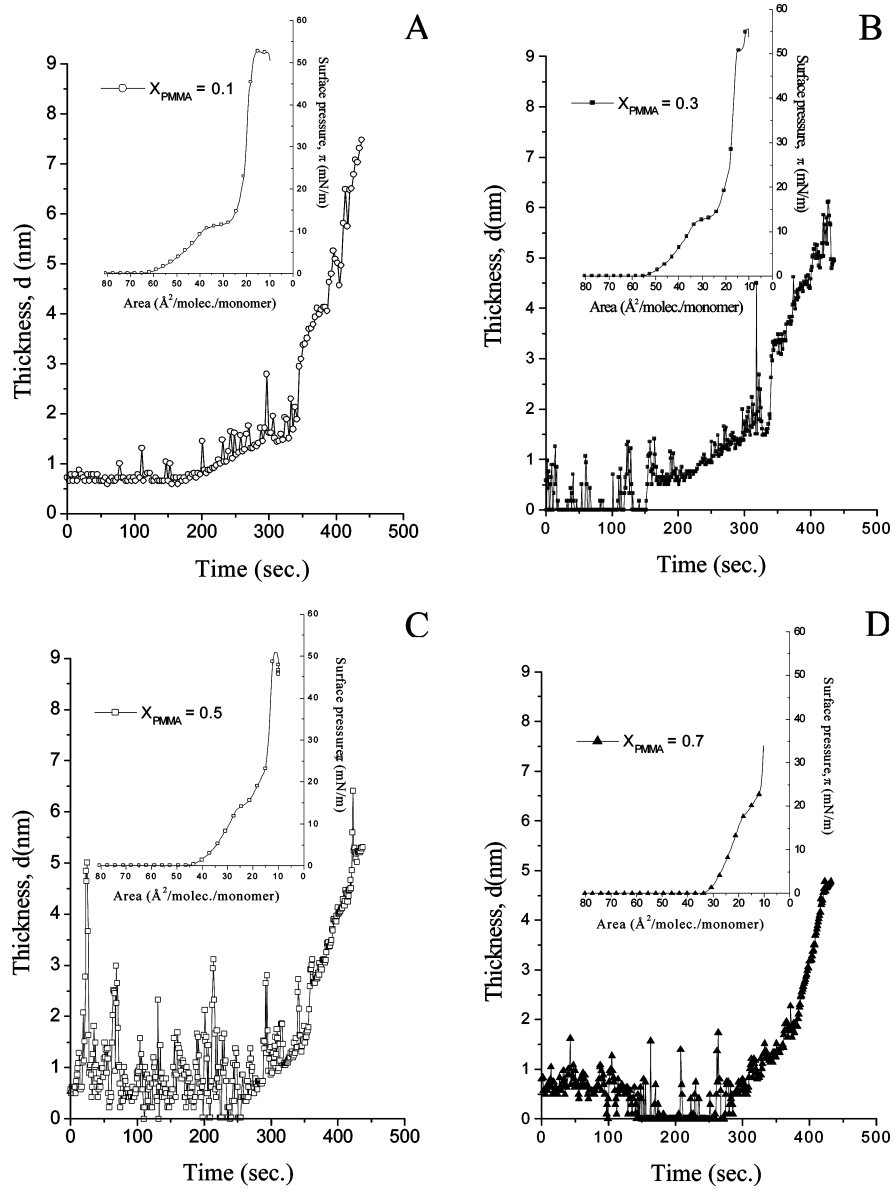

Figure 6. Thickness versus time plots corresponding to PMMA (M_w = 15 000)−monopalmitin mixed monolayers spread on water at pH = 6 and 30 °C: (A) X_{PMMA} = 0.1; (B) X_{PMMA} = 0.3; (C) X_{PMMA} = 0.5; (D) X_{PMMA} = 0.7. Insets: π−A isotherms relative to these mixed monolayers.

As the amount of polymer increases in the mixtures, their thickness (at the end of the compression) diminishes from a value around of approximately 7 nm when X_{PMMA} is 0.1−4.75 nm when X_{PMMA} is 0.7. Therefore, increasing the amount of PMMA in mixed monolayers causes a decrease in their thickness. This behavior seems logical if we take into account the smaller size of the polymer hydrophobic chains compared to those of the lipid.

During the first stages of compression, the thickness of all mixed films is about 0.5 nm, irrespective of their composition. Under these conditions, the monolayers exhibit a *gas−liquid expanded* (G−LE) phase transition and their isotherms show a constant-surface pressure plateau of approximately 0 mN/m (insets of Figure 6), as it corresponds to a horizontal orientation of both molecules on the water surface. When the surface pressure exerted by the monolayer starts to increase (as a result of the *liquid-expanded* surface phase formation), the thickness of the mixed films also increases considerably, from a 0.5 nm initial value to a higher one (1.5−2 nm), according to the composition of the mixtures. In this region, the BAM images obtained are homogeneous, as shown in Figure 7A, for the mixture composition X_{PMMA} = 0.1, obtained at a surface pressure of 3.9 mN/m.

Once the LE−LC phase transition is reached, the thickness of the mixed films increases again (Figure 6) and the resulting BAM images show the existence of numerous star-like domains, consisting of 4−5 lobes (Figure 7B), typical of lipid monolayers in this transition region.[11] These domains are gradually blurred, lose losing their "star-like" configuration and show a more diffuse appearance as the polymer proportion increases in the mixtures (Figure 7C,D).

After the LE−LC phase transition, the monolayer thickness increases considerably as it is compressed (Figure 6). This increase in thickness is evidenced by the presence of more or less compact domains in the BAM images, depending on the composition of the mixed film (Figure 7E−G).

Finally, when the monolayer collapses, a number of noise peaks are observed in the thickness curves (Figure 6), which correspond to the 3D phases involved in this state, evidenced in detail in the BAM images of Figure 7H−J.

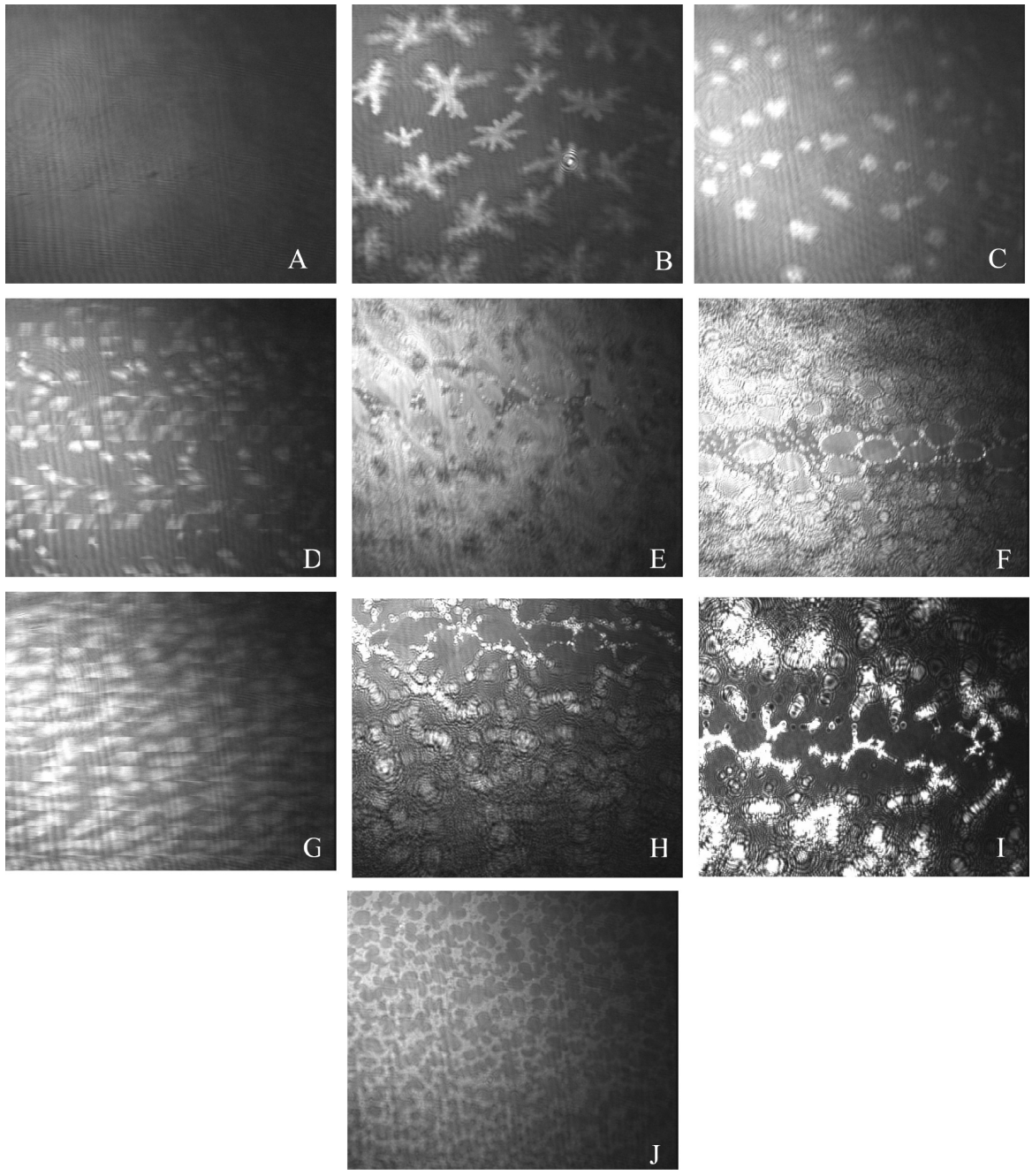

Figure 7. Visualization of PMMA (M_w = 15 000)−monopalmitin monolayers spread at the air−water interface at pH 6 and 30 °C for Brewster angle microscopy: (A) $X_{PMMA} = 0.1$, $\pi = 3.9$ mN/m; (B) $X_{PMMA} = 0.1$, $\pi = 10.5$ mN/m; (C) $X_{PMMA} = 0.3$, $\pi = 11.5$ mN/m; (D) $X_{PMMA} = 0.5$, $\pi = 14.1$ mN/m; (E) $X_{PMMA} = 0.1$, $\pi = 16.2$ mN/m; (F) $X_{PMMA} = 0.3$, $\pi = 21.7$ mN/m; (G) $X_{PMMA} = 0.5$, $\pi = 19.8$ mN/m; (H) $X_{PMMA} = 0.1$, $\pi = 50$ mN/m; (I) $X_{PMMA} = 0.3$, $\pi = 54$ mN/m; (J) $X_{PMMA} = 0.7$, $\pi = 52$ mN/m.

4. Discussion

4.1. PMMA (120 000)−Monopalmitin Mixtures. In general, the results obtained in the study of the PMMA (120 000)−monopalmitin system lead to the following conclusions:

1. Both $\pi-A$ isotherms and $C_s^{-1}-\pi$ curves (Figures 1 and 2) show the existence of two phase transitions in mixed monolayers of $X_{PMMA} \leq 0.5$: the first, at a surface pressure of about 14.5 mN/m (similar to that of monopalmitin) and the second at 20−21 mN/m surface pressures (slightly higher than that of PMMA). In addition, all mixed films exhibit two well-differentiated collapses: one corresponding to the lipid film (at surface pressures of 50−51 mN/m) and the other one related to that of PMMA, at surface pressures of about 57−58 mN/m.

2. The plots of the mean molecular areas occupied by the mixed monolayers as a function of the mole fraction of PMMA show the existence of positive deviations from linearity when the surface pressure at which the areas are measured is lower than 15 mN/m, that is, below the first phase transition of the monolayers. The maximum deviation is reached in the mixture of $X_{PMMA} = 0.7$ (Figure 8, where the excess areas of mixed films versus mole fraction of PMMA were plotted), which corresponds to an "*azeotropic* mixture" made of poly(methylmethacrylate) and monopalmitin in an approximate molecular relation of 2:1 PMMA/Mp.

The bibliography contains different interpretations to explain the existence of these positive excess areas. Thus, in several papers on mixed monolayers of paclitaxel (taxol) and phospholipids, the authors[12−14] consider that the positive deviations from the ideality ideal behavior are due to the fact that the intermolecular forces between the components of the mixture

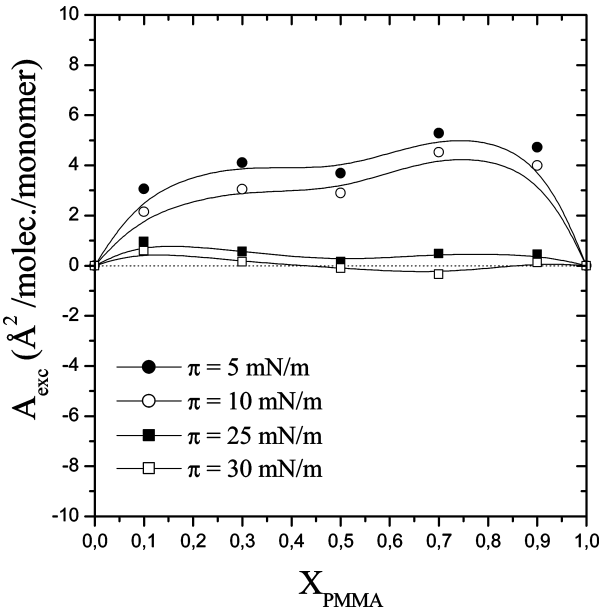

Figure 8. Plots of the excess area of mixing vs mole fraction of PMMA (M_w = 120 000) at various surface pressures Corresponding to PMMA−Mp mixed monolayers spread on water at pH 6 and 30 °C.

are lower than those between the pure components; that is, adding one component to another causes a weakening of the molecular interactions as a result of the geometric accommodation of the voluminous taxol molecule in the hydrocarbon chains of phospholipid. The different orientation of the components of the mixture[15] or the steric hindrance caused by a particular component are the arguments often pointed out to explain the positive deviations.[16,17] In other cases, these deviations are attributed to the existence of repulsive electrostatic interactions between the polar groups of molecules,[18−20] to their solvation[21] or to the formation of molecular aggregates (clusters).[22]

In our PMMA−Mp system, the monoplamitin glycerol group is not ionized under working conditions (pH = 6), and neither is the polar group of PMMA (methyl ester group); therefore, an explanation for the positive deviations from the ideality ideal behavior based on the existence of repulsive interactions between the polar groups is unlikely. On the contrary, such polar groups should have some attractive interactions, as a result of the possible formation of hydrogen bonds between them.

Therefore, a possible interpretation for the positive deviations from the ideal behavior could be based on the existence of a change in PMMA conformation, as suggested by Peng and Barnes.[23] It can be stated that at low surface pressures the monopalmitin molecules, more or less horizontally oriented on the water surface, interact with the polymeric lattice and thus cause an unfolding of the PMMA molecules from the coiled arrangement in the pure PMMA monolayer (where, due to steric hindrance, it can be argued that some monomer units must be out the surface) to a flatter configuration with most monomer units at the surface. Partial areas per monomer unit of PMMA can give some information on the existence of these changes in the polymer conformation. From the data in Figure 3, partial areas can be calculated by the method of intercepts: the intersection with the Y axis at $X_{PMMA} = 1$ of the tangent to the $A_m - X_{PMMA}$ curve at a given composition provides the value of the partial area of the PMMA, whereas the intersection with the Y axis at $X_{PMMA} = 0$ allows determining the value of the partial area of monopalmitin. In the range of mole fractions X_{PMMA} = 0.1−0.7, the values corresponding to the mean

TABLE 3: Characteristic Parameters for PMMA (M_w = 120 000) and Monopalmitin Mixed Monolayers[a]

	$\bar{A}$		A_0		ΔA	
	5 mN/m	10 mN/m	5 mN/m	10 mN/m	5 mN/m	10 mN/
PMMA	22.1	19.8	16.0	14.2	6.1	5.6
monopalmitin	51.2	43.5	48.5	41.4	2.7	2.1

[a] $\bar{A}$: partial areas per monomer unit at surface pressures of 5 and 10 mN/m. A_0: mean areas per monomer unit. ΔA: difference between them.

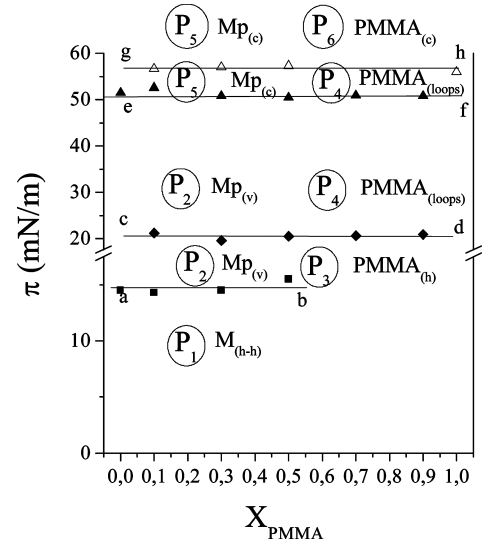

Figure 9. Phase diagram corresponding to PMMA (M_w = 120 000)−monopalmitin mixed monolayers spread on water at 30 °C and pH 6. $M_{(h-h)}$ corresponds to a mixed monolayer consisting of PMMA and Mp molecules, both horizontally oriented to the air−water interface, forming a miscible system. $Mp_{(v)}$ denotes vertically oriented molecules of monopalmitin. $PMMA_{(h)}$ and $PMMA_{(loops)}$ correspond to PMMA horizontally oriented molecules and forming loops, respectively. $Mp_{(c)}$ and $PMMA_{(c)}$ denote collapsed states of both components.

molecular areas lie on a straight line (Figure 3), yielding values for PMMA partial areas of 22.1 Å^2/monomer at 5 mN/m and 19.8 Å^2/monomer at π = 10 mN/m. The comparison between these values and the area per monomer for the pure PMMA (16 and 14.2 Å^2/monomer, respectively) (Table 3) shows that the partial area for PMMA mixed with monopalmitin is about 6 Å^2 higher than when is pure. However, when determining the partial molecular areas of monopalmitin, the obtained values (where 51.2 Å^2/molecule at 5 mN/m and 43.5 Å^2/molecule at 10 mN/m) are only about 2.5 Å^2 higher than the area occupied by pure monopalmitin (48.5 Å^2/molecule at 5 mN/m and 41.4 Å^2/molecule at 10 mN/m), that is, lower than half the PMMA values. Consequently, positive deviations from the ideality ideal behavior of PMMA−Pm mixed monolayers can be attributed to a change from the coiled conformation configuration of PMMA at low surface pressures, to a flatter conformation configuration.

Using the phase diagram of Figure 9, and applying the Crisp phase rule:[24,25] $P = C - F + 1$ to the transition and collapse regions observed in PMMA−Mp mixed monolayers (values shown in Table 1), the number of surface phases at the equilibrium and the miscibility or immiscibility of the film-forming components in the mixed system can be determined. So, the application of this rule to the first phase transition leads to the existence of three phases in equilibrium along the line a−b. Actually, in this situation, the number of components, C, is 2 (PMMA and Mp) and the degrees of freedom, F, are 0,

since the surface pressure at the transition region is maintained at a constant value irrespective of the change in the composition. Consequently, on the a−b horizontal line in Figure 9 three phases (P) in equilibrium are coexistent:

Phase P_1, consisting of PMMA and Mp molecules, both horizontally oriented on the air/water interface, forming a miscible system ($M_{(h\text{-}h)}$) at surface pressures below 15 mN/m. Under these conditions, the $A-X_{PMMA}$ plots show positive deviations from ideal behavior (Figures 3 and 5), confirming the miscibility of the mixture components.

Phase P_2, consisting of monopalmitin molecules which, as a result of the LE−LC phase transition carried out at 14.5 mN/m, change their orientation from a horizontal position (*liquid−expanded state*) to a vertical position (*liquid−condensed state*) ($Mp_{(v)}$). This orientation change provokes their immiscibility with the horizontally oriented PMMA horizontally oriented, The incompatibility of the components due to their different orientation in the interface is often reported in the literature.[26−34]

Phase P_3, consisting of PMMA molecules horizontally oriented on the water surface ($PMMA_{(h)}$), which, in accordance with the above-mentioned remarks, form an immiscible phase with the P_2.

When compressed, the mixed monolayers undergo a second phase transition at surface pressures of 20−21 mN/m, which is attributed to a change of the PMMA molecular conformation configuration from a flatter to a coiled configuration due to the folding of the polymer segments, forming loops at the interface.[35] Applying the phase rule to the system under the conditions corresponding to this second transition (line c−d of Figure 8) shows, in the same way as explained above, the existence of three equilibrium phases: *phases P_2* and *P_3*, described above, and a new *phase P_4* made up of the looplike bent polymer ($PMMA_{(loops)}$), which is also immiscible with the vertically oriented monopalmitin oriented vertically. The fact that the plots of the mean molecular areas, as a function of the composition, are linear at 25 and 30 mN/m surface pressures, as shown in Figure 3, confirms the immiscibility of the components in this region of the monolayer.

When the first collapse is reached at 50−51 mN/m, monopalmitin is expelled from the mixed film to form a three-dimensional *phase*, *P_5*, constituted by collapsed Mp collapsed ($Mp_{(c)}$), which is in equilibrium with P_2 and P_4 phases. Since the value of this collapse pressure remains constant throughout the range of compositions (line d−e), $F = 0$, and as a result the application of the phase rule gives rise to the existence of three equilibrium phases ($P = 3$), which we have just described above.

Finally, during the second collapse at 57−58 mN/m (line f−g), the expelling of the PMMA molecules from out of the monolayer occurs, resulting in the corresponding three-dimensional *phase P_6*, formed by collapsed PMMA collapsed ($PMMA_{(c)}$) in equilibrium with P_4 and P_5 phases. Again, the application of the phase rule leads to the existence of three equilibrium phases under these conditions.

4.2. PMMA (15 000)−Monopalmitin Mixtures. The fact that the positive deviations from linearity of the molecular areas are lower for the PMMA (M_w = 15 000)−Mp system (Figure 5) than for the PMMA (M_w = 120 000)−Mp mixtures (Figure 3) can be attributed to the full extension of the polymer (M_w = 15 000) molecules on the water surface (at low surface pressure) in relation to the coiled arrangement of the PMMA (M_w = 120 000) monolayer[35] under these conditions. So, the monopalmitin provokes a smaller conformation configuration change in the polymer (M_w = 15 000), thus causing a lower positive deviation from linearity.

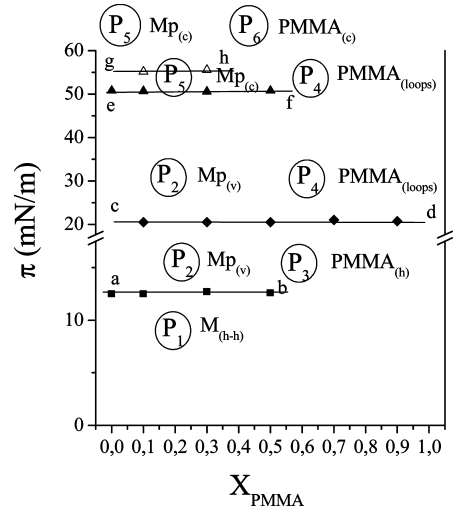

Figure 10. Phase diagram corresponding to PMMA (M_w = 15 000)−monopalmitin mixed monolayers spread on water at 30 °C and pH = 6. $M_{(h\text{-}h)}$ corresponds to a mixed monolayer consisting of PMMA and Mp molecules, both horizontally oriented to the air−water interface forming a miscible system. $Mp_{(v)}$ denotes vertically oriented molecules of monopalmitin. $PMMA_{(h)}$ and $PMMA_{(loops)}$ correspond to PMMA horizontally oriented molecules and forming loops, respectively. $Mp_{(c)}$ and $PMMA_{(c)}$ denote collapsed states of both components.

The phase diagram of PMMA (M_w = 15 000)−monopalmitin mixtures obtained from the data in Table 2 (deduced from the results for the $C_s^{-1}-\pi$ curves in Figure 4) is shown in Figure 10. The only difference related to the results obtained with the polymer of 120 000 molecular weight lies in the numerical values for the different phase transitions, which are slightly different from one system to another. Regardless of these small differences, the obvious fact is that the surface behavior of the mixture components is the same in both cases. Therefore, the discussion put forward in the previous section can be applied entirely to the PMMA (M_w = 15 000)−Mp system.

5. Conclusions

PMMA−Mp mixed monolayers ($X_{PMMA} \leq 0.5$) exhibit two phase transitions shown by two discontinuities in the corresponding $\pi-A$ isotherms and by two minimum values in $C_s^{-1}-\pi$ curves: the first transition, at a surface pressure of about 14.5 mN/m (similar to that of monopalmitin) and the second at 20−21 mN/m surface pressures (slightly higher than that of PMMA). In addition, all mixed films exhibited two well-differentiated collapses: one corresponding to the lipid film (at surface pressures of 50−51 mN/m) and the other one related to that of PMMA, at surface pressures of about 57−58 mN/m. Using the phase diagram and applying the Crisp phase rule to these transition and collapse regions, the number of surface phases at the equilibrium and the miscibility or immiscibility of the film-forming components in the mixed system were determined. Besides, the plot of the mean molecular areas occupied by the mixed monolayers as a function of the mole fraction of PMMA showed the existence of positive deviations from linearity when the surface pressure at which the areas were measured is lower than 15 mN/m, that is, below the first phase transition of the monolayers. This was attributed to the unfolding caused at low surface pressures by the Mp on PMMA molecules, provoking the change of their coiled arrangement in the pure PMMA monolayer to a flatter configuration in the mixed film.

At higher surface pressures, the areas per monomer unit of the mixed monolayers obey the additivity rule, which was attributed to the fact that the film components form an immiscible system in these conditions.

Acknowledgment. We acknowledge the support of the Xunta de Galicia (Spain) through the Project number PGIDIT07PXIB-203133PR.

Note Added after ASAP Publication. This article was published ASAP on February 2, 2010. Figure 1 has been modified. The correct version was published on February 8, 2010.

References and Notes

(1) Plazonnet, B. *Modified-release drug delivery technology in Ophthalmic drug delivery*; Rathbone, M. J., Hadgraft, J., Roberts, M. S., Ed.; Marcel Dekker Inc.: New York, 2003; pp 289−313.
(2) Sander, B.; Van Best, J.; Johansen, S.; et al. *Curr. Eye Res.* **2003**, *27*, 247.
(3) Reddy, I. K., Ganesan, M. G. In *Ocular therapeutics and drug delivery: an overview*; Reddy, I. K., Ed.; Technomic Publishing Co.: Lancaster, PA, 1999; pp 3−29.
(4) Myles, M. E.; Neumann, D. M.; Hill, J. M. *Adv. Drug Deliv. Rev.* **2005**, *57*, 2063.
(5) Shah, C.; Raj, S.; Foulks, G. N. *Ophthalmol. Clin. N. Am* **2003**, *16*, 95.
(6) Alvarez Lorenzo, C.; Hiratani, H.; Concheiro, A. *Am. J. Drug Deliv.* **2006**, *4* (3), 131.
(7) Vandorselaer, T.; Youssfi, H.; Caspers-Vain, L. E.; et al. *J. Fr. Ophthalmol.* **2001**, *24*, 1025.
(8) Lesher, G. A.; Gunderson, G. G. *Optom. Vis. Sci.* **1993**, *70*, 1012.
(9) Salz, J. J.; Reader, A. L.; Schwartz, L. J.; et al. *J. Refract. Corneal Surg.* **1994**, *10*, 640.
(10) Hsu, W. P.; Lee, Y. L.; Liou, S. H. *Appl. Surf. Sci.* **2006**, *252*, 4312.
(11) Miñones, J., Jr.; Rodríguez Patino, J. M.; Conde, O.; Carrera, C.; Seoane, R. *Colloids Surf. A* **2002**, *203*, 273.
(12) Feng, S. S.; Gong, K.; Chew, J. *Langmuir* **2002**, *18*, 4061.
(13) Zhao, L.; Feng, S. S.; Go, M. L. *J. Pharm. Sci.* **2002**, *93*, 86.
(14) Zhao, L.; Feng, S. S. *J. Colloid Interface Sci.* **2004**, *274*, 55; **2005**, *285*, 326.
(15) Cadenhead, D. A.; Benedikt, M. J.; Kellner, K. J.; Papahadjopoulos, D. *Biochemistry.* **1977**, *16*, 5386.
(16) Grainger, D. W.; Reichert, A.; Ringsdorf, H.; Salesse, C.; Davies, D. E.; Lloyd, J. B. *Biochim. Biophys. Acta* **1990**, *1022*, 146.
(17) Rosilio, V.; Kasselouri, A.; Albrecht, G.; Baszkin, A. *Prog. Colloid Polym. Sci.* **1997**, *103*, 294.
(18) Sáchez González, J.; Cabrerizo Wilches, M. A.; Gálvez Ruiz, M. J. *Colloids Surf. B.* **2001**, *21*, 19.
(19) Abrioul, H.; Sánchez González, J.; Maqueda, M.; Gálvez, A.; Valdivia, E.; Gálvez Ruiz, M. J. *J. Colloid Interface Sci.* **2001**, *233*, 306.
(20) Korchowicz, B.; Paluch, M. *Prog. Colloid Polym. Sci.* **1997**, *105*, 103.
(21) Gong, K.; Feng, S. S.; Go, M. L.; Soew, P. H. *Colloids Surf. A* **2002**, *207*, 113.
(22) Maget-Dana, R. *Biochim. Biophys. Acta* **1999**, *1462*, 109.
(23) Peng, J. B.; Barnes, G. T. *Langmuir* **1991**, *7*, 3090.
(24) Crisp, D. J. *Surface Chemistry (Supplement Research)*; Butterworth: London, 1949; pp 17−35.
(25) Defay, R., Prigogine, I., Bellmans, A., Everett, D. E. *Surface Tension and Adsorption*; Longmans Green and Co.: London, 1966; p 71.
(26) Gabrielli, G. *J. Colloid Interface Sci.* **1975**, *53*, 148.
(27) Gabrielli, G.; Maddi, A. *J. Colloid Interface Sci.* **1978**, *64*, 19.
(28) Gabrrielli, G.; Puggelli, M.; Baglioni, P. *J. Colloid Interface Sci.* **1982**, *86*, 4585.
(29) Puggelli, M.; Gabrielli, G. *Colloid Polym. Sci.* **1983**, *261*, 82; **1987**, *263*, 879; **1987**, *265*, 432.
(30) Niccolai, A.; Baglioni, P.; Dei, L.; Gabrielli, G. *Colloid Polym. Sci.* **1989**, *267*, 262.
(31) Malcolm, B. R. *Progress in Surface and Membrane Science*; Academic Press Inc.: New York, 1973; vol. 7; p 223.
(32) Ries, H. E.; Walter, D. C. *J. Colloid Interface Sci.* **1961**, *16*, 361.
(33) Dörfler, H. D.; Koth, C.; Rettig, W. *Langmuir* **1995**, *11*, 4803.
(34) Dörfler, H. D.; Koth, C.; Rettig, W. *J. Colloid Interface Sci.* **1996**, *180*, 487.
(35) Miñones, J., Jr.; Miñones Conde, M.; Yebra-Pimentel, E.; Trillo, J. M. *J. Phys. Chem.* **2009**, *113*, 17455.

JP907900G